Supporting Information

A Flexible NHC-Aryloxido Aluminum Complex and Its Zwitterionic Imidazolium Aluminate Precursor in Ring-Opening Polymerization of ε-Caprolactone.

Santu Goswami,[a] Pranay Mandal,[a,#] Subham Sarkar,[a,b,#] Mainak Mukherjee,[c] Samanwita Pal,[c] Dibyendu Mallick,[b,*] Debabrata Mukherjee[a,*]

[a] Department of Chemical Sciences, Indian Institute of Science Education and Research Kolkata Mohanpur, Nadia, 741246, India.

[b] Department of Chemistry, Presidency University, 86/1 College Street, Kolkata, 700073, India.

[c] Department of Chemistry, Indian Institute of Technology Jodhpur, Karwar, Rajasthan 342037, India

Table of Contents

1. Spectroscopic Characterization:

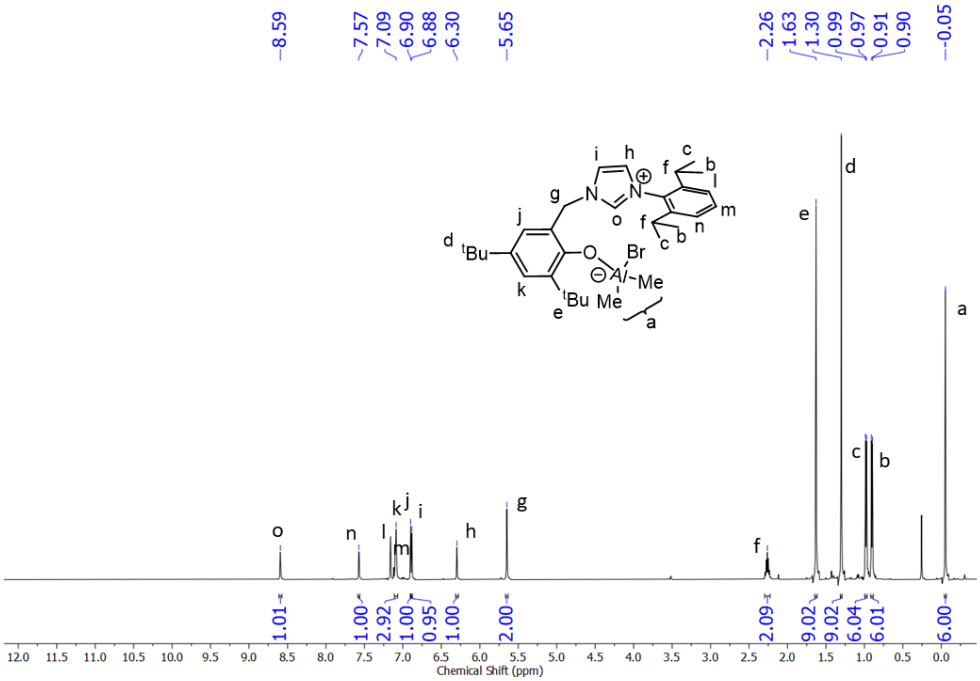

Figure S1: ^{1}H NMR spectrum of 1 in benzene-*d*$_6$/THF-*d*$_8$ (5:1).

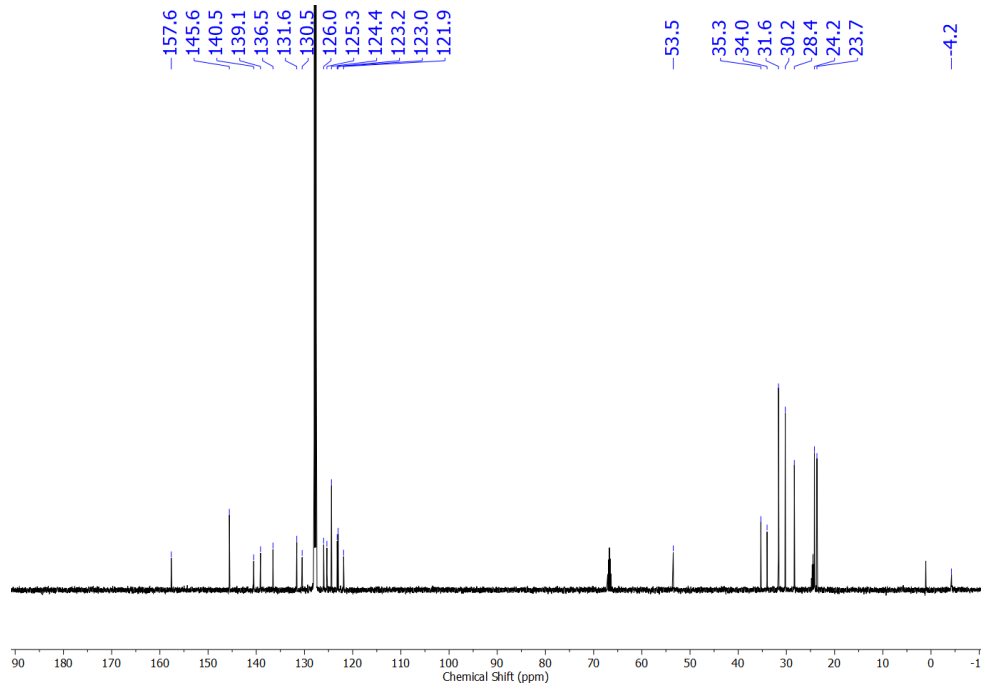

Figure S2: ^{13}C{^{1}H} NMR spectrum of 1 in benzene-*d*$_6$/THF-*d*$_8$ (5:1).

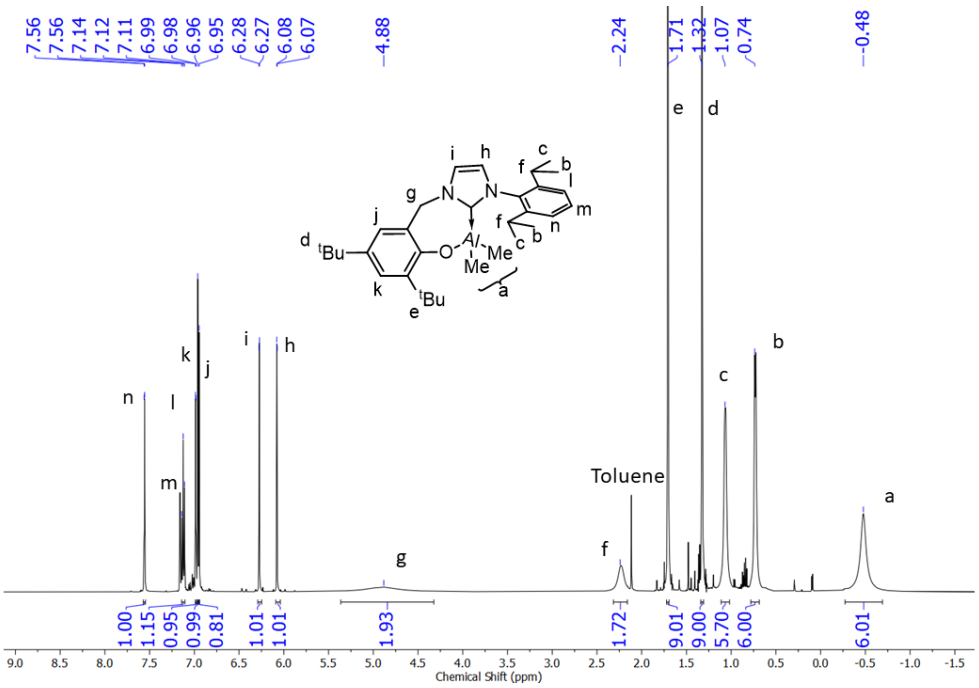

Figure S3: ^{1}H NMR spectrum of 2 in benzene-d_6 at room temperature.

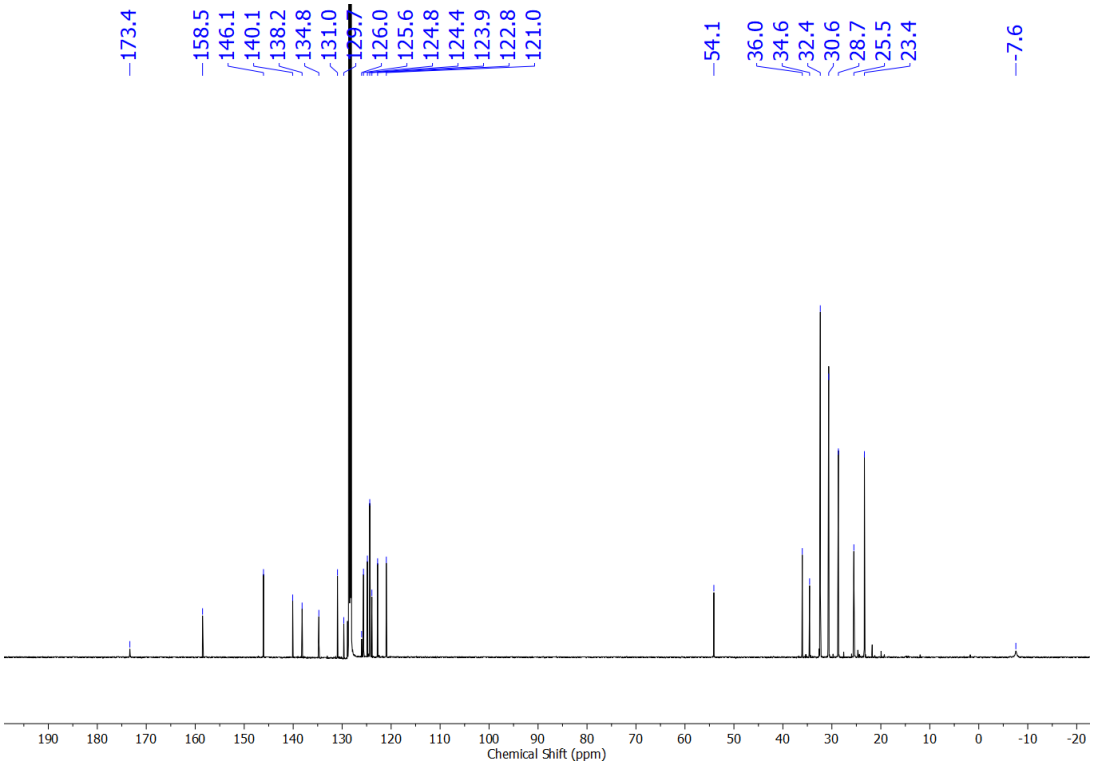

Figure S4: ^{13}C{^{1}H} NMR spectrum of 2 in benzene-d_6 at room temperature.

2. Variable temperature ^{1}H NMR spectra and line-shape Analyses:

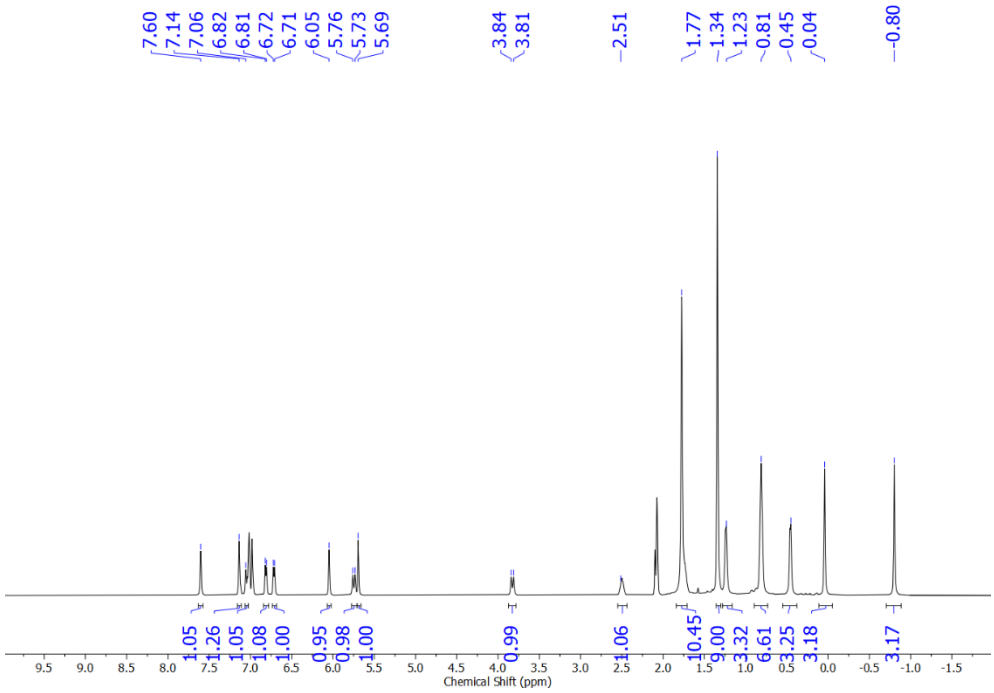

Figure S5: ^{1}H NMR spectrum of 2 in toluene-d_8 at recorded at – 60 ^{o}C.

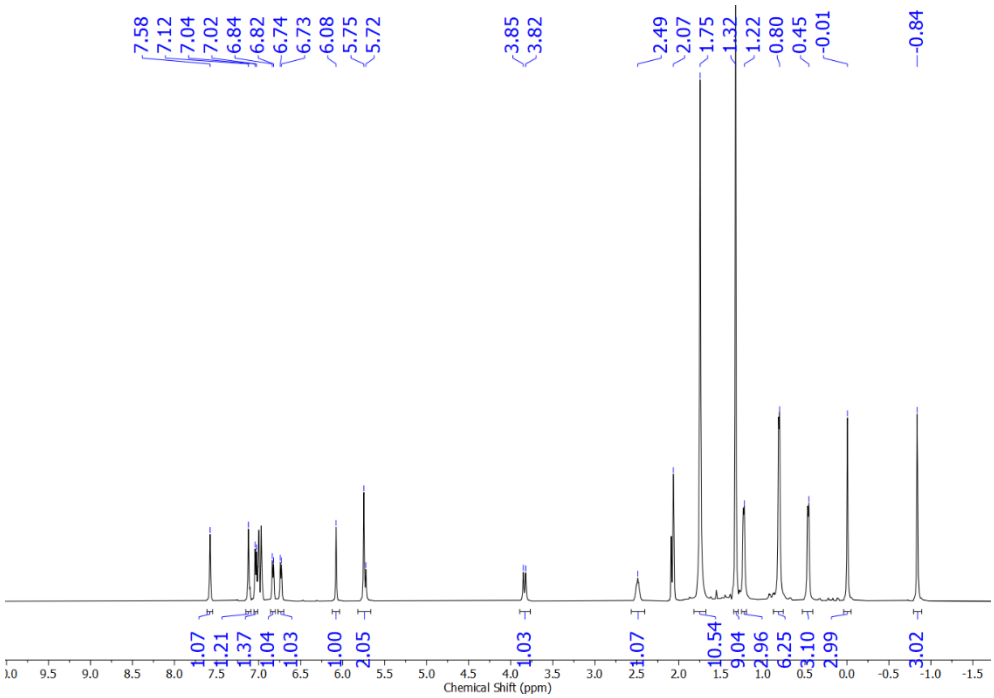

Figure S6: ^{1}H NMR spectrum of 2 in toluene-d_8 at recorded at – 50 ^{o}C.

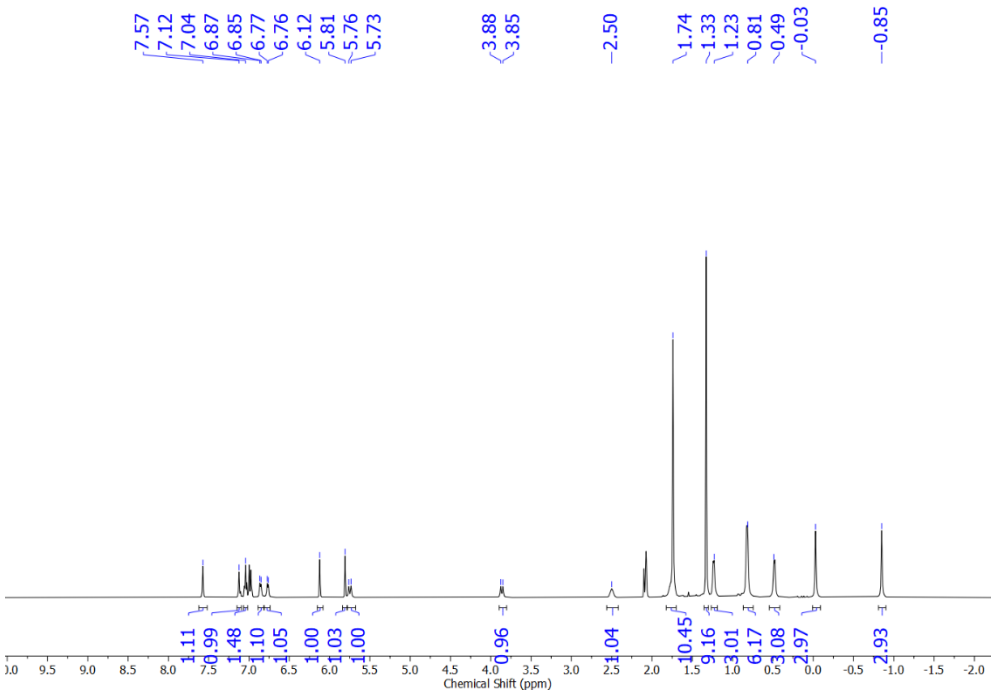

Figure S7: ^{1}H NMR spectrum of 2 in toluene-d_8 at recorded at – 40 ^{o}C.

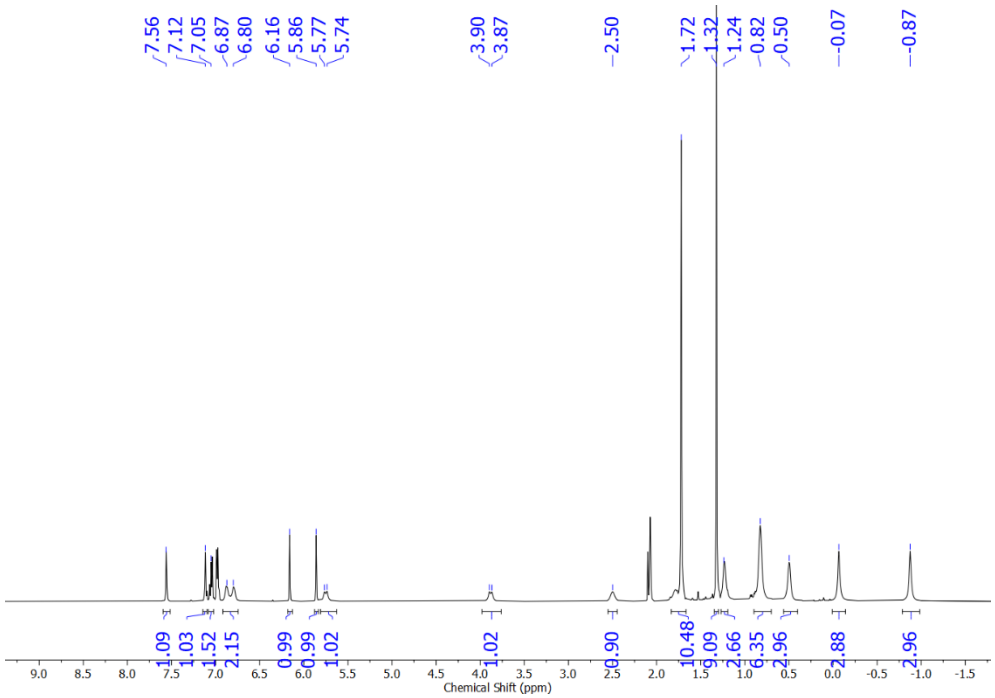

Figure S8: ^{1}H NMR spectrum of 2 in toluene-d_8 at recorded at – 30 ^{o}C.

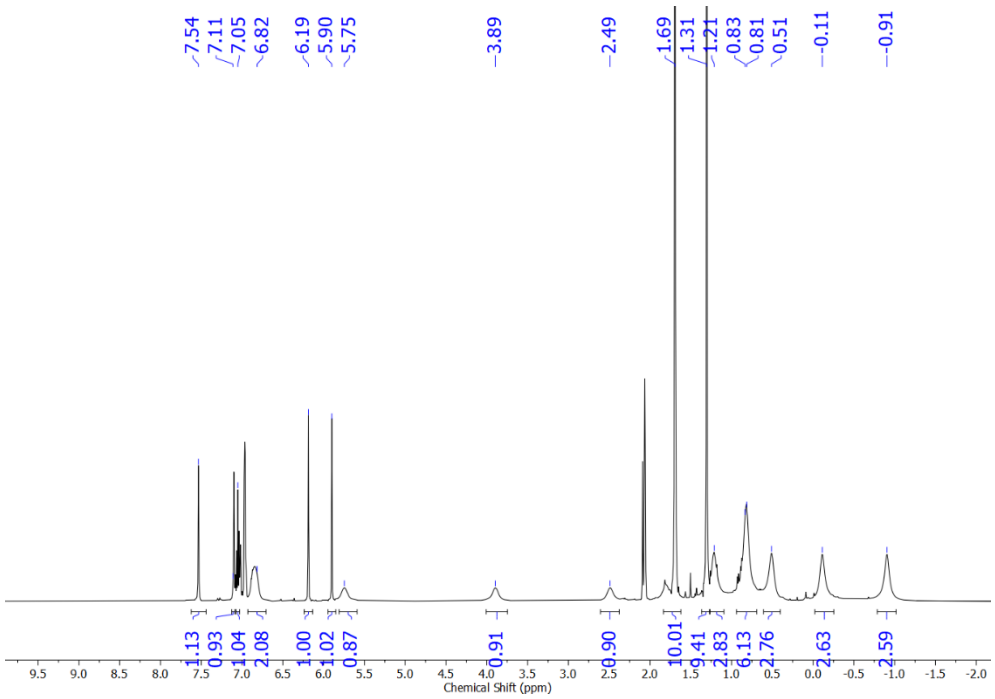

Figure S9: ^{1}H NMR spectrum of 2 in toluene-d_8 at recorded at – 20 ^{o}C.

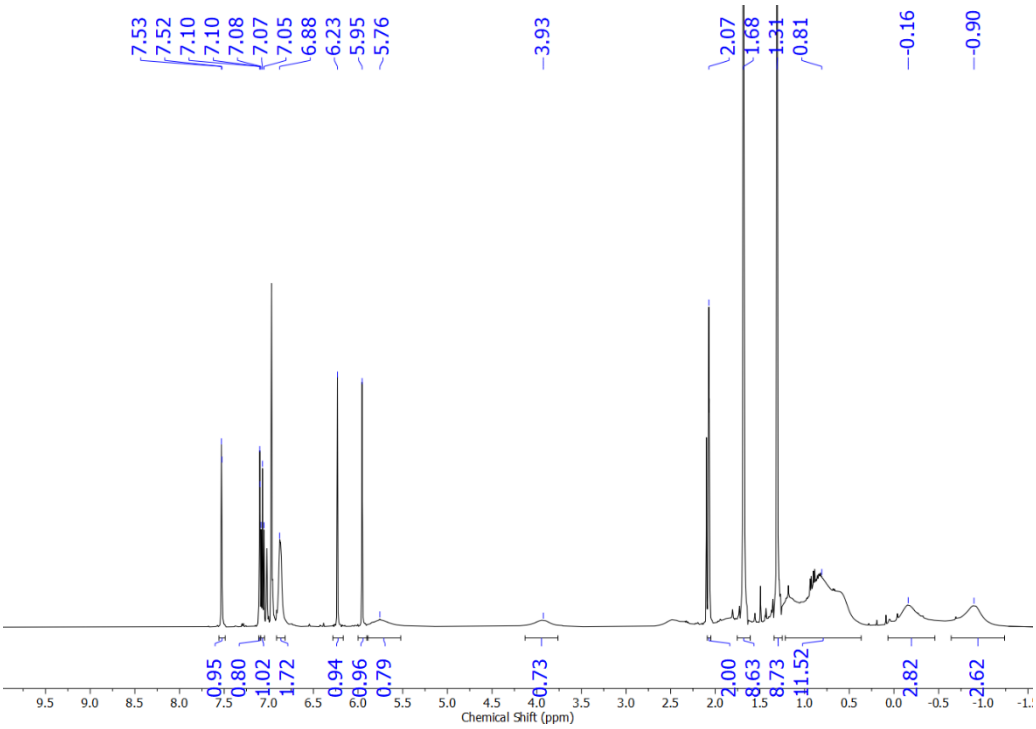

Figure S10: ^{1}H NMR spectrum of 2 in toluene-d_8 at recorded at – 10 ^{o}C.

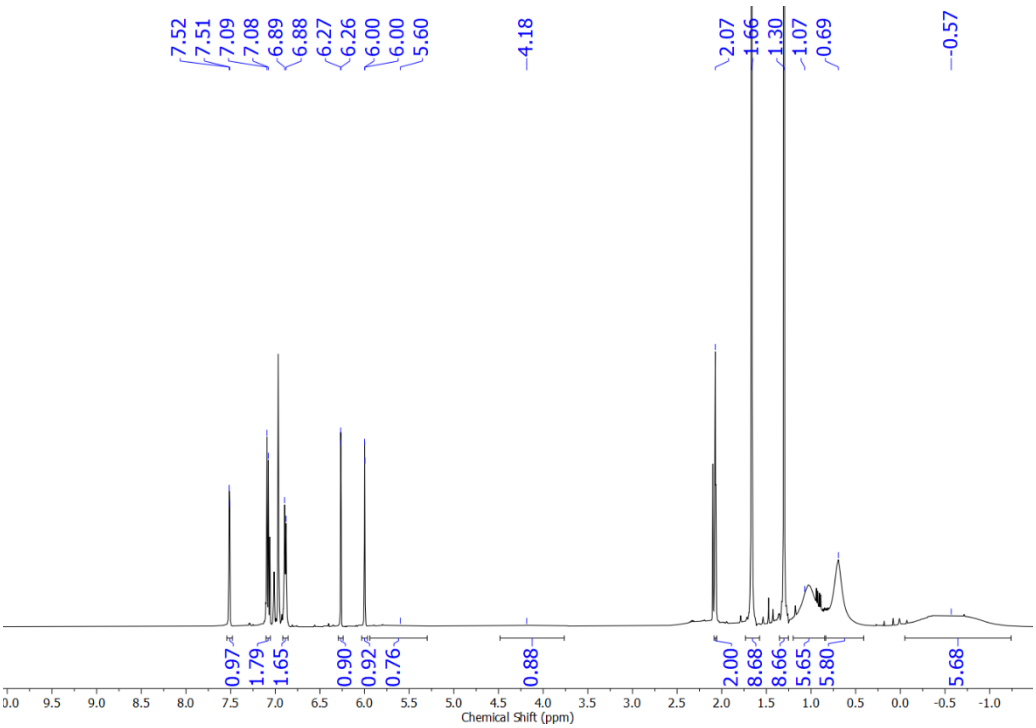

Figure S11: ^{1}H NMR spectrum of 2 in toluene-d_8 at recorded at 0 ^{o}C.

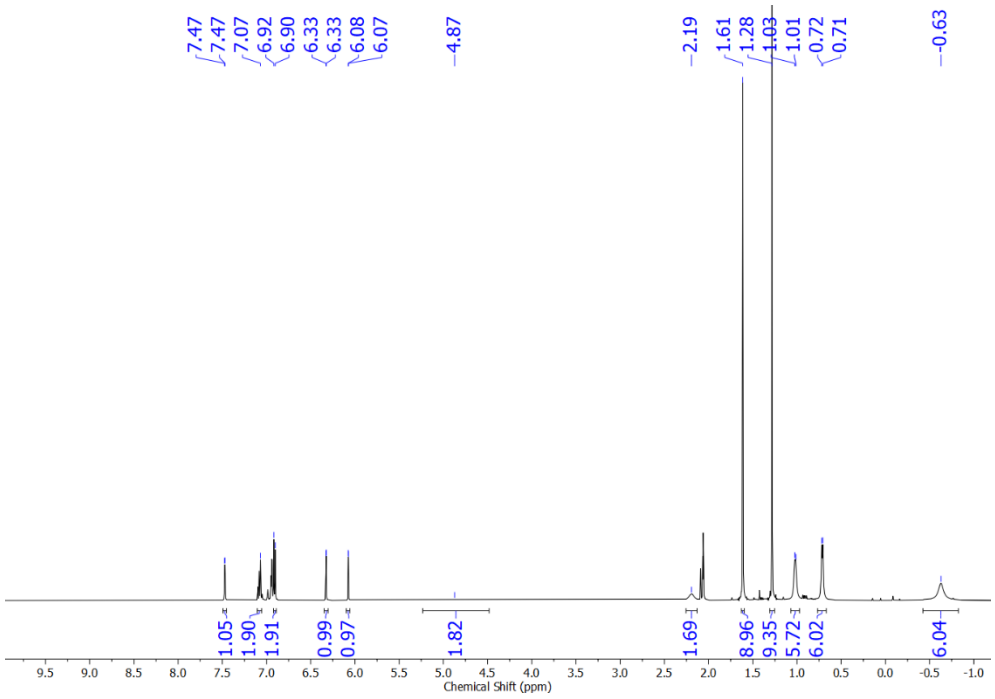

Figure S12: ^{1}H NMR spectrum of 2 in toluene-d_8 at recorded at 25 ^{o}C.

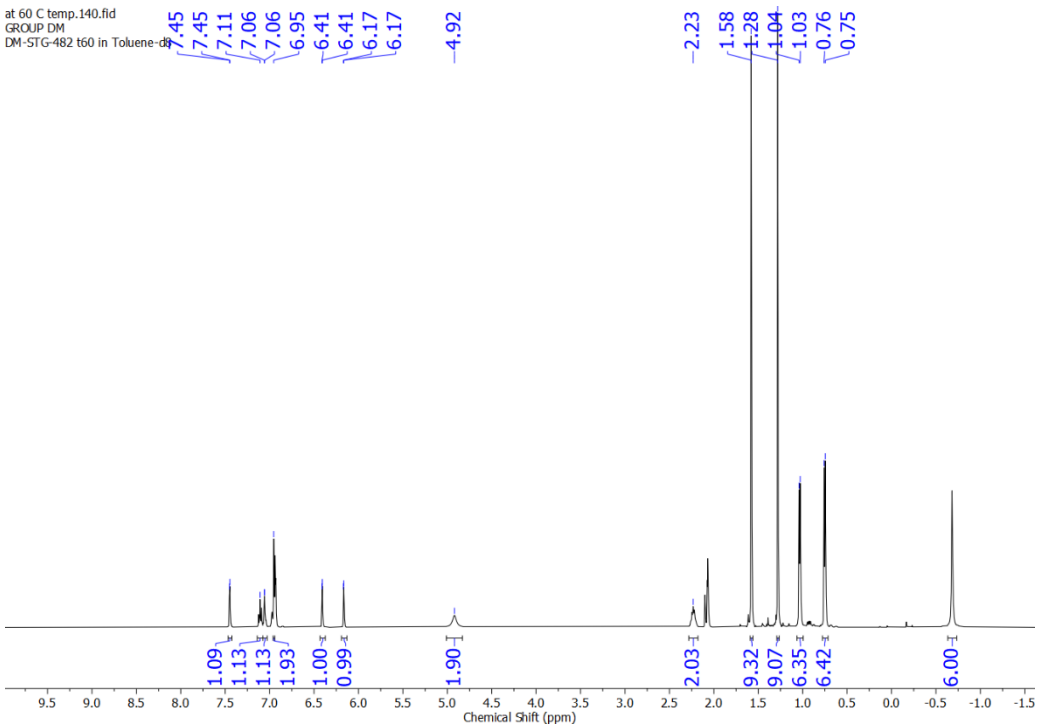

Figure S13: ^{1}H NMR spectrum of 2 in toluene-d_8 at recorded at 60 ^{o}C.

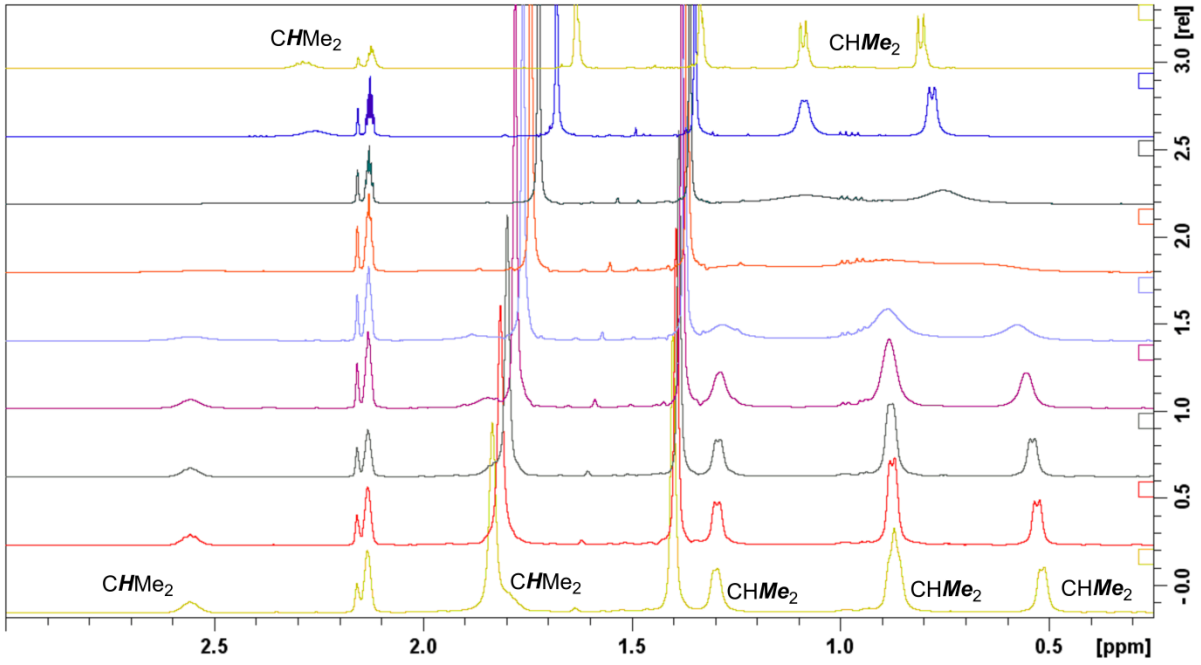

Figure S14: A stacked plot showing the variable temperature ^{1}H NMR spectra of 2 in toluene-d_8 focussing on the Dipp-C*H*Me$_2$ resonances.

Line-shape Analysis

A complete line-shape analysis has been carried out following literature report to extract the rate constants for the chemical exchange processes identified by the VT NMR measurements. Two cases were considered: a) two site exchange involving uncoupled exchanging sites (AlMe2) and b) two site exchange involving coupled exchanging sites (CH2). For both the cases appropriate equations are used as represented by equation S1 and S2. Further WinDNMR

software is used to simulate the exchange phenomena and the respective simulated exchange spectra and the corresponding exchange rate constants are presented in figure S15.

For Methyl Group:

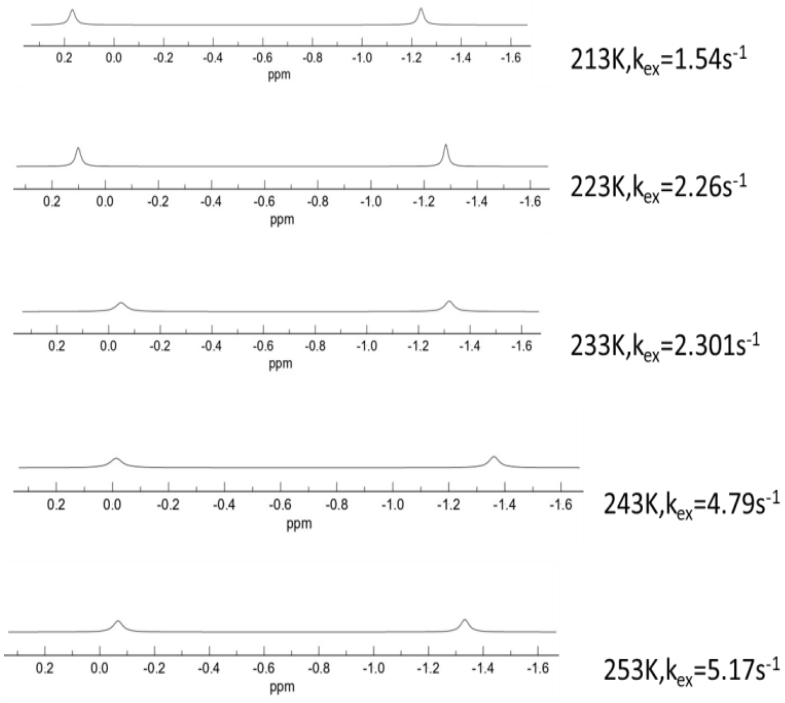

For Hydrogen (Coupled Spin-System)

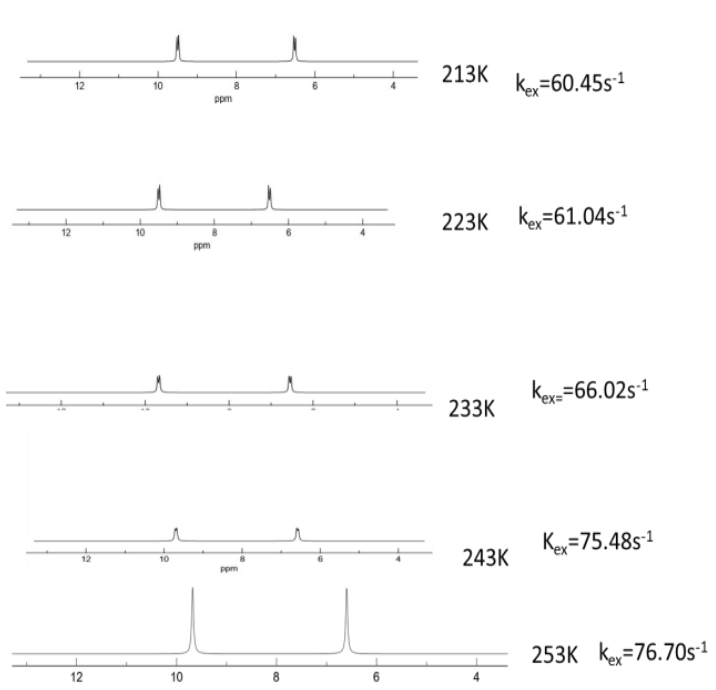

Figure S15: Stack plots of simulated VT-^{1}H NMR spectra of 2 showing the Al*Me*$_2$ (*top*) and -C*H*$_2$- (*bottom*) regions. The spectra are generated using WinDNMR software [*Note that the chemical shift scale in the WinDNMR generated spectra varies from the experimental spectra in some cases, however the chemical shift difference between the two exchanging sites is perfectly matching with the experimental spectra]

The following equations are used for extraction of exchange rates:

$$k = \frac{\pi}{\sqrt{2}} \times \Delta\vartheta \quad \text{.....(S1)}$$

(where $\Delta\vartheta$ is the change of the line width (Full Width Half Maxima) in Hz between the two uncoupled exchanging sites.)

Whereas for the hydrogens, coupled two site exchange is considered and equation S2 is used to extract the exchange rate constant:

$$k = \frac{\pi}{\sqrt{2}} \times \sqrt{\Delta\vartheta^2 + 6\,{J_{AB}}^2} \quad \text{.....(S2)}$$

(Where J_{AB} is the mutual coupling constant between A and B sites)

213 K is considered as the temperature where the exchange process is practically frozen. Eyring equation is used to extract the thermodynamic parameters. Figure S16 represents the corresponding Eyring plots for AlMe2 (Figure S16, *left*) and CH2 groups (Figure S16, *right*).

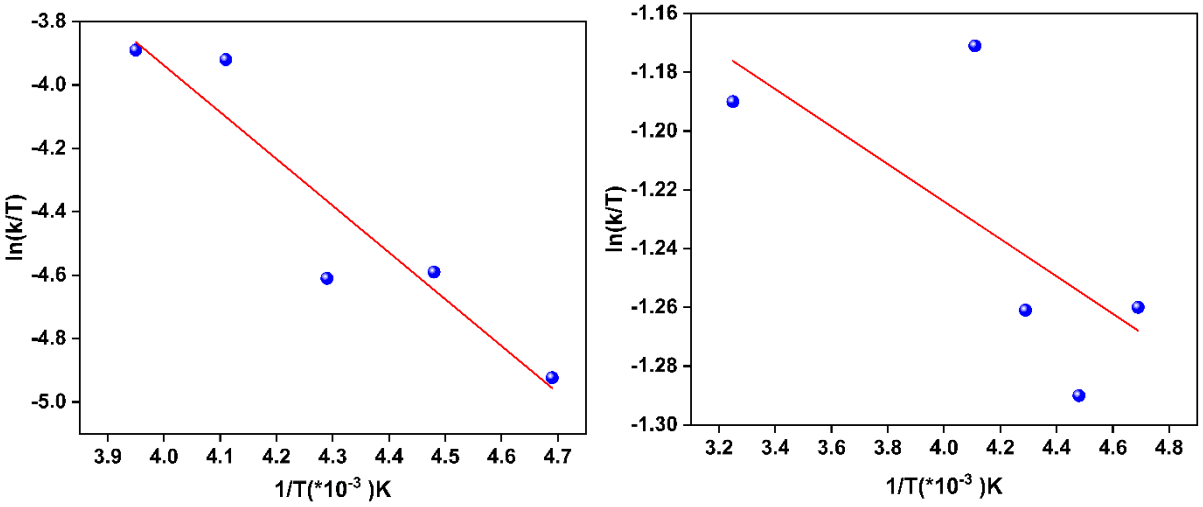

Figure S16: Eyring plots of the two Al-*Me* Groups (*left*) and the CH_2 protons (*right*).

Determination of the Thermodynamic Parameters (Enthalpy & Entropy) by Eyring Equation:

$$\ln\left(\frac{k}{T}\right) = -\frac{\Delta H^{\ddagger}}{R}\left(\frac{1}{T}\right) + \ln\left(\frac{k_B}{h}\right) + \frac{\Delta S^{\ddagger}}{R}$$

($\Delta H^{\ddagger}$ & $\Delta S^{\ddagger}$ are enthalpy of activation and entropy of activation, respectively)

Table: S1: Thermodynamic parameters (derived from Eyring Plots)

Chemical Group	Enthalpy(ΔH)	Entropy(ΔS)
Methyl (AlMe2)	12.221 KJ/mole	-181.35 J/K
Proton (CH2)	0.49884 KJ/mole	-24.73 J/K

3. PCL analyses and control experiments:

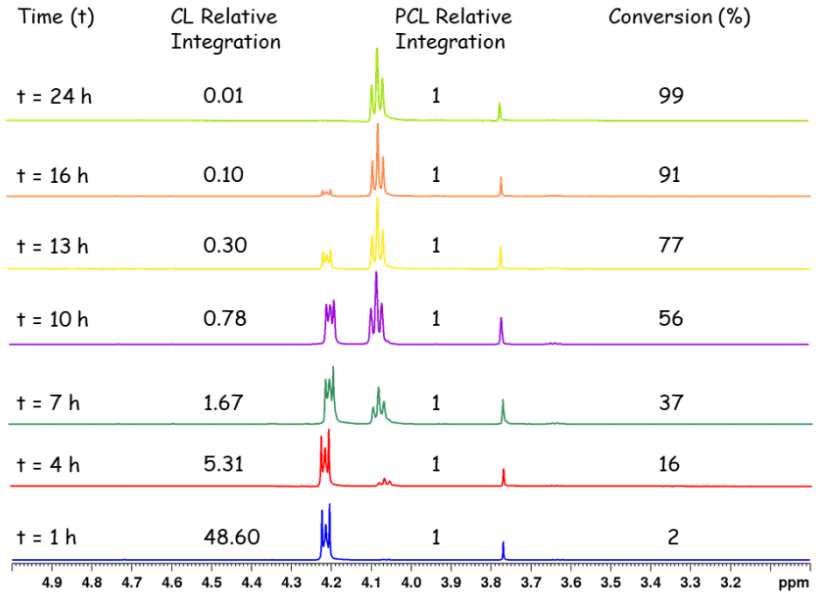

Figure S17: Monitoring the % conversion [(PCL integration)/[(PCL integration) + (CL integration)] × 100] over time by ^{1}H NMR spectra for a ROP catalysis with [CL]/[2]/[BnOH] in 100:1:2 ratio in toluene at room temperature. 1,3,5-Trimethoxybenzene is used as an internal standard.

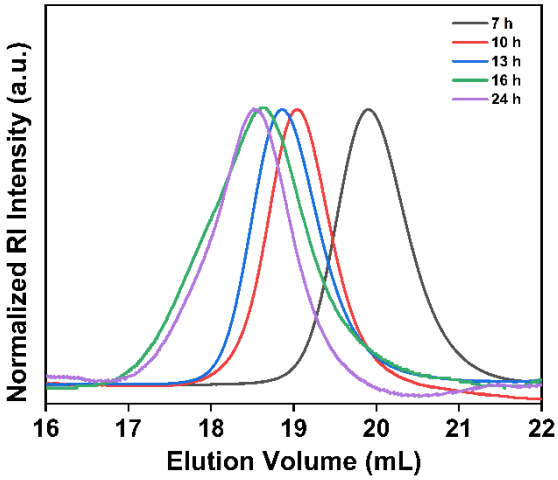

Figure S18: SEC RI traces of the PCLs obtained at different time intervals for [CL]/[2]/[BnOH] as 100:1:2.

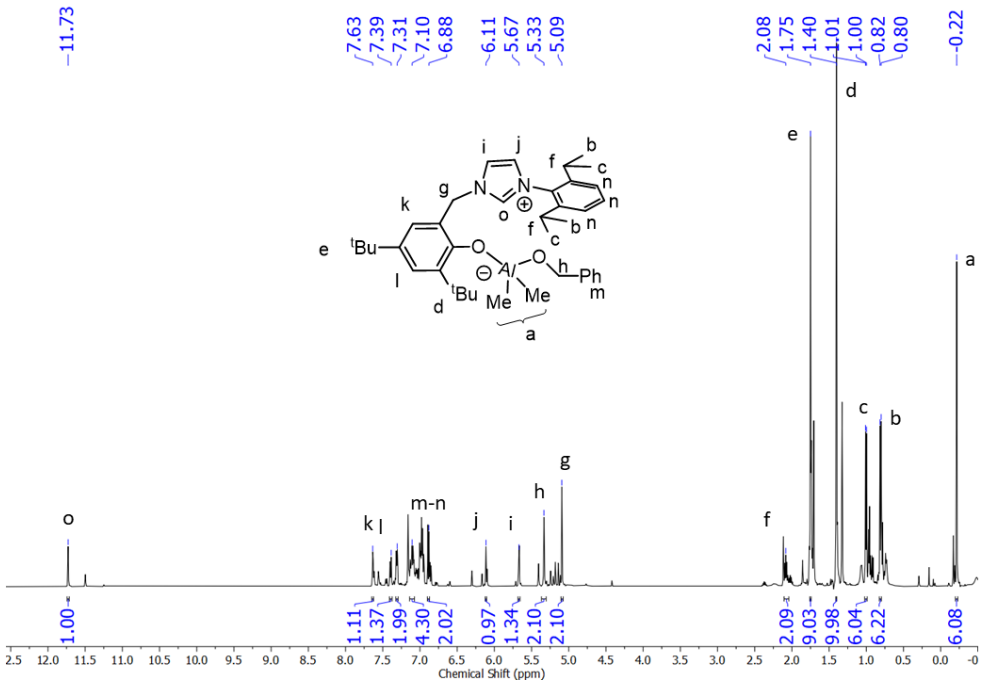

Figure S19: ^{1}H NMR spectrum measured in situ for the 1:1 reaction between 2 and BnOH in benzene-d_6. The appearance of an imidazolium-2-*H* and the retention of the $AlMe_2$ groups are clearly visible.

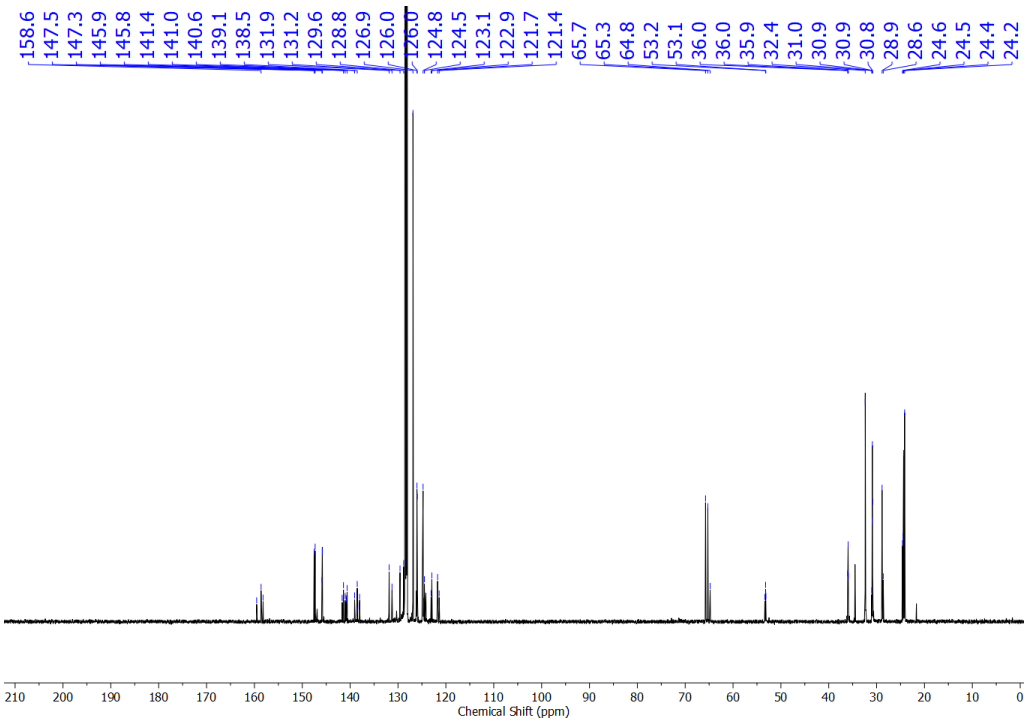

Figure S20: $^{13}C\{^{1}H\}$ NMR spectrum measured in situ for the 1:1 reaction between 2 and BnOH in benzene-d_6. The δ_{NHC} resonance disappears to suggest the carbene protonation.

Table S2: Comparison of relative rates for the PCL runs with [CL]:2:BnOH as 100:1:*x* (*x* = 1, 2, 3).

[CL]/2/BnOH	Entry	Time (h)	Conversion (%)
100:1:2	1	6	13
	2	10	56
	3	13	77
	4	16	91
	5	24	99
100:1:1	6	6	10
	7	12	60
	8	16	90
	9	24	98
100:1:3	10	6	15
	11	12	65
	12	16	92
	13	24	99

Oligomerization analysis:

For the run of [CL]/2/BnOH as 5:1:2.

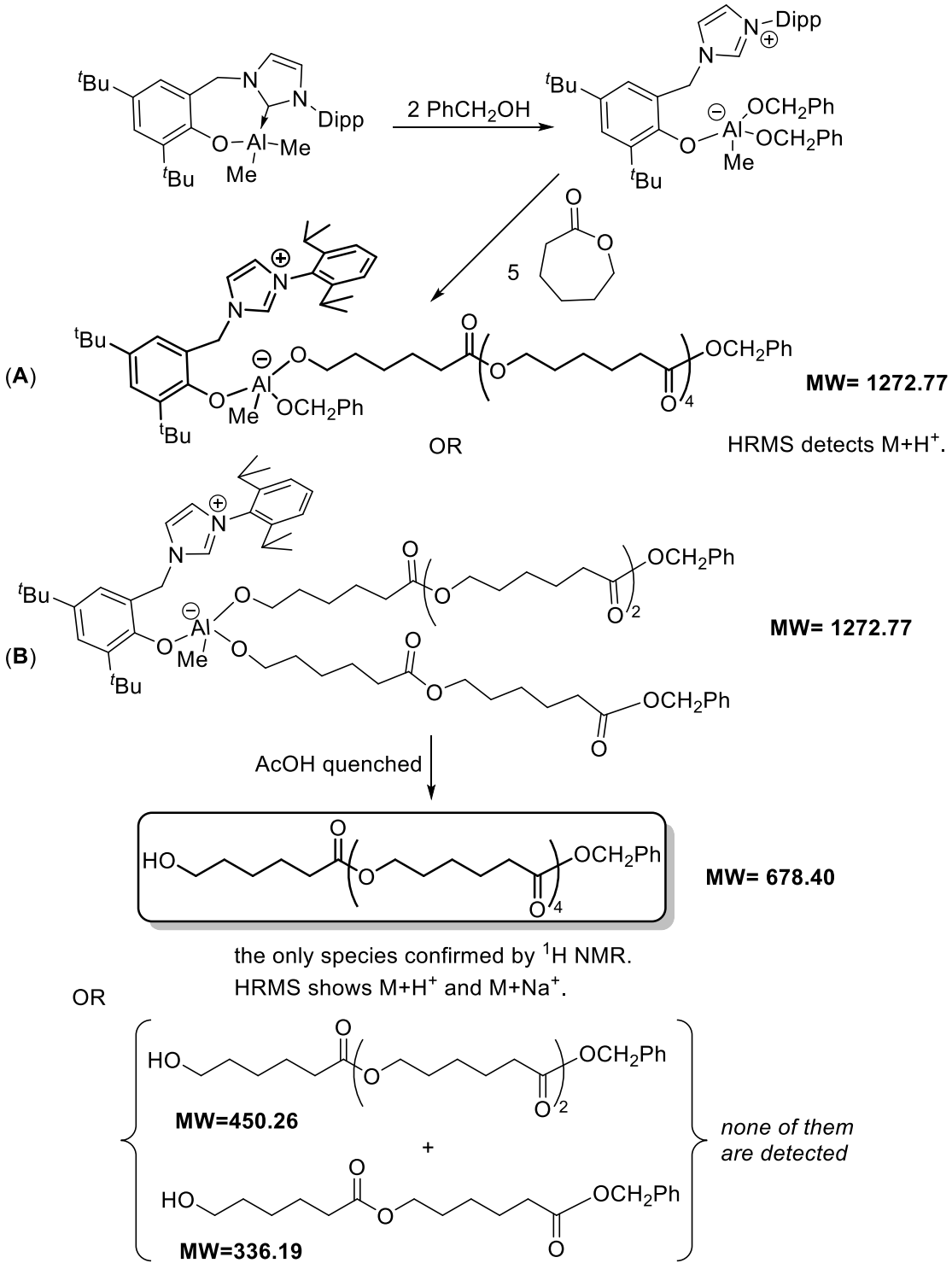

Scheme S1: The oligomerization analysis considering the possibilities of a single propagating chain vs. a double propagating chain. Masses of the two complexes before quenching would be identical and hence won't be distinguishable by HRMS. But had there been more than one propagating chain, that would have reflected in the ^{1}H NMR and HRMS data, which is clearly not the case here. Only the pentamer with -OBn as the end group is detected.

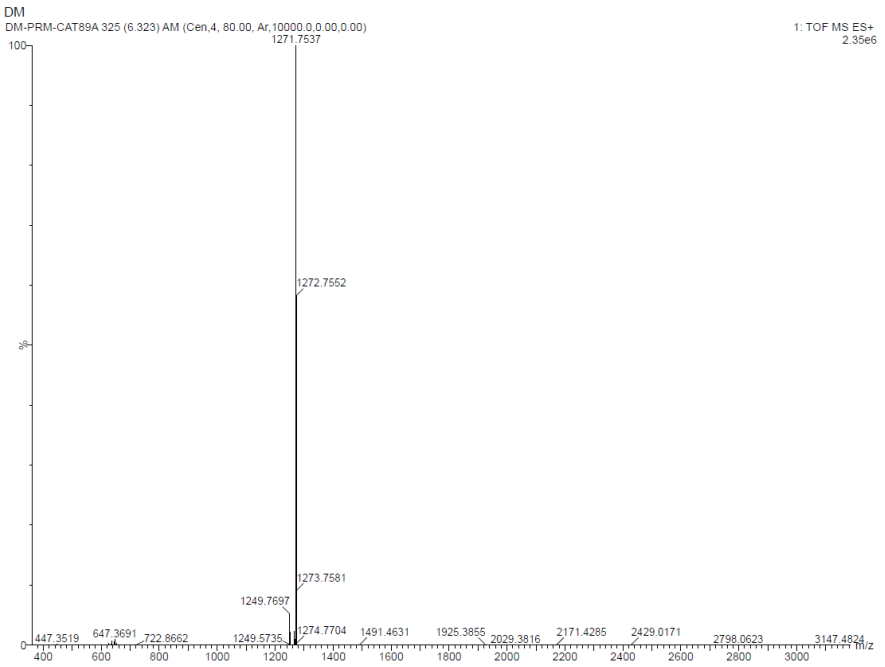

Figure S21: HRMS data showing the proposed Al-complex (A; Scheme S1) upon ring-opening of five CLs.

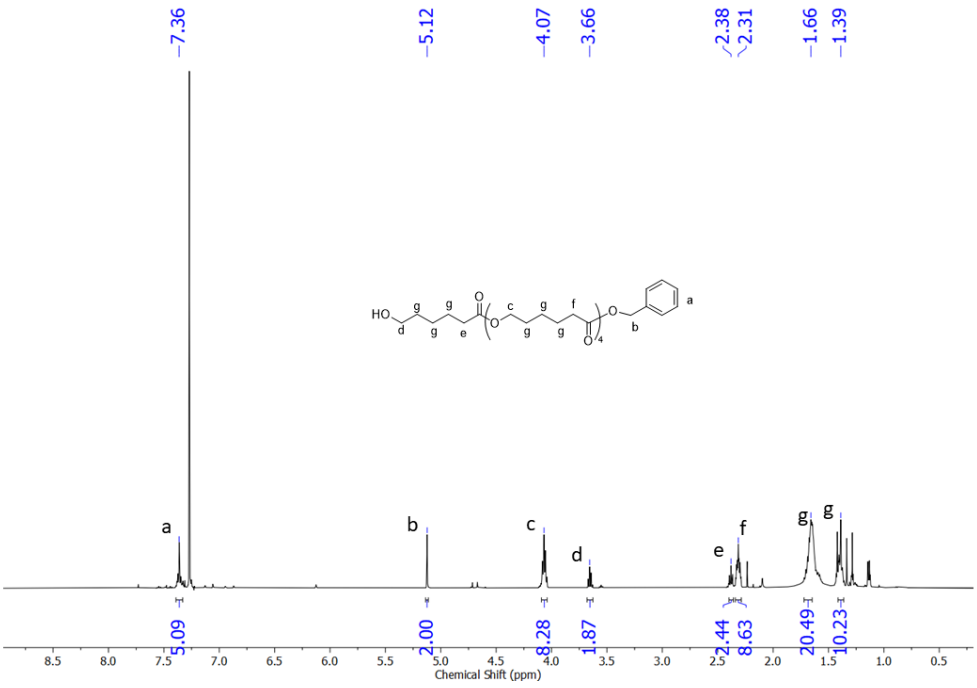

Figure S22: ^{1}H NMR spectrum after quenching showing the expected linear pentamer with a -OBn terminal group. Note: The pentamer stays soluble in methanol/hexane mixture and couldn't be purified by precipitation. As the result, the ^{1}H NMR spectrum shows some minor impurities.

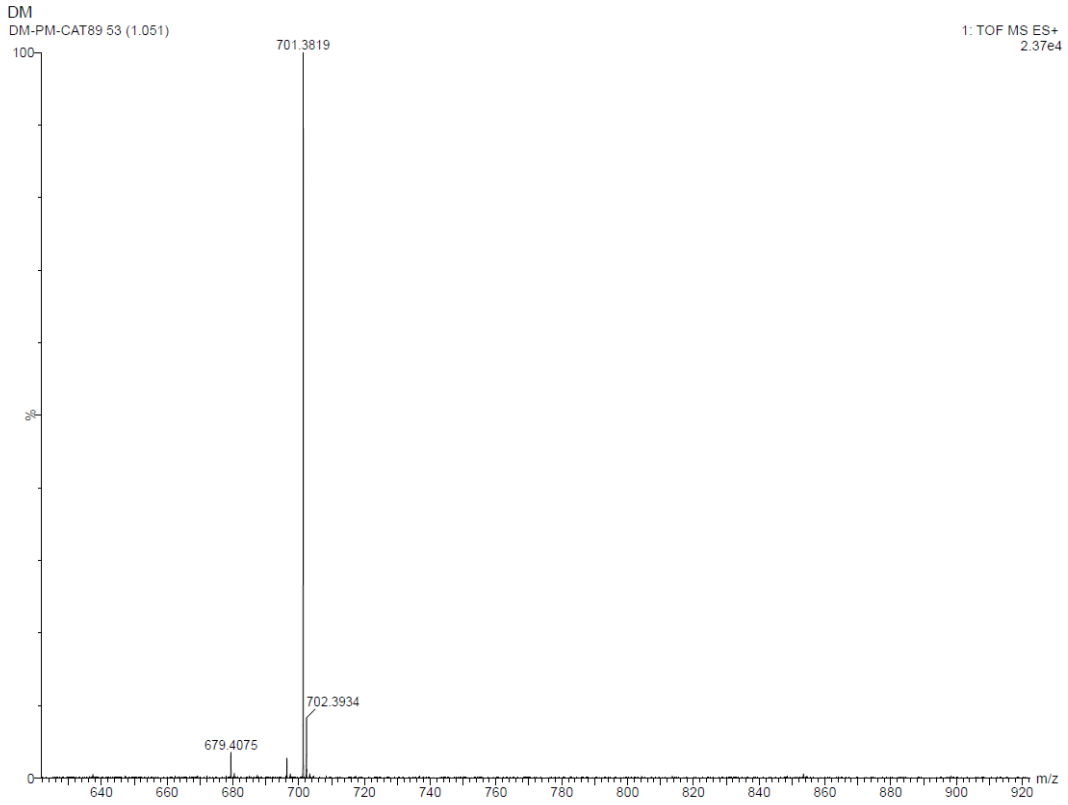

Figure S23: HRMS data after quenching showing the pentameric CL with -OBn as the end group. The data show M+H$^+$ and M+Na$^+$.

For the run of [CL]/2/BnOH as 10:1:2.

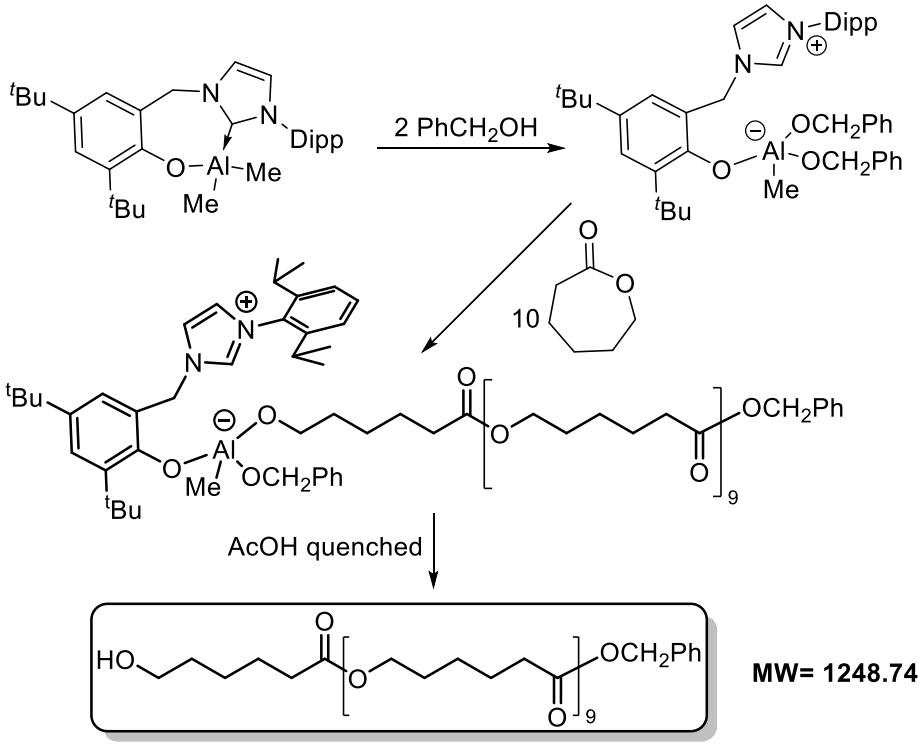

the only species confirmed by ^{1}H NMR.
HRMS shows M+H$^+$ and M+Na$^+$.

Scheme S2: The oligomerization analysis considering the possibility of a single propagating chain. Mass of the decamer with -OBn as the end group is detected after quenching (see Fig. S26).

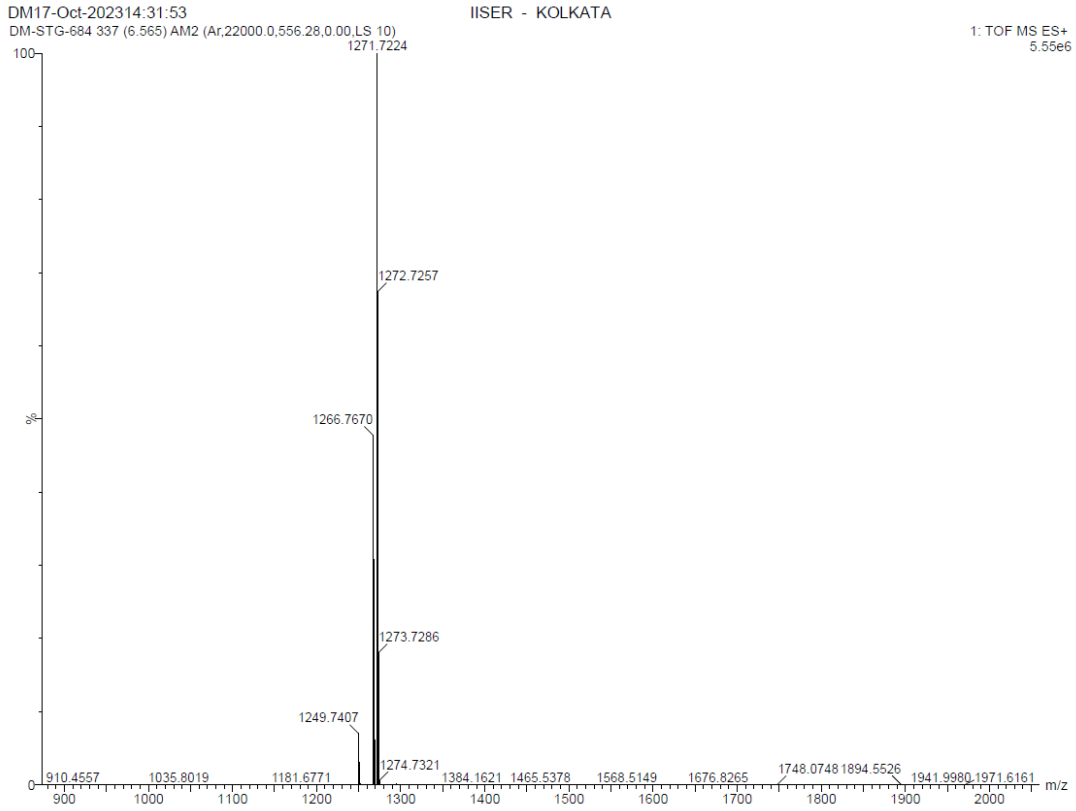

Figure S24: HRMS data after quenching showing the decameric CL with -OBn as the end group. The data show $M+H^+$ and $M+Na^+$.

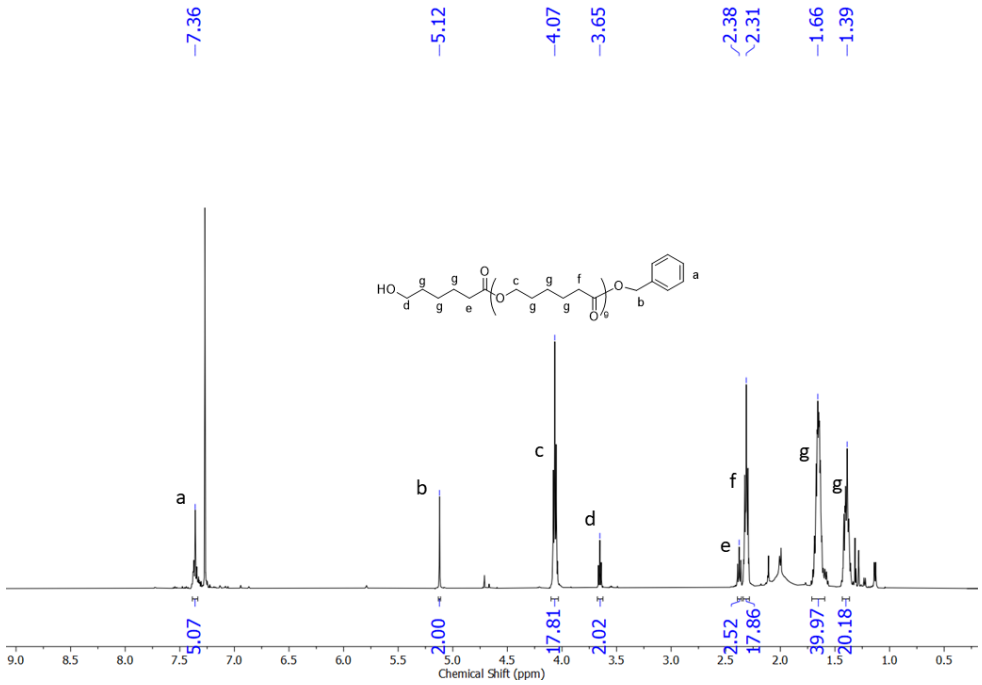

Figure S25: ^{1}H NMR spectrum showing the expected linear decamer with a -OBn terminal group. Note: The decamer stays soluble in methanol/hexane mixture and couldn't be purified by precipitation. As the result, the ^{1}H NMR spectrum shows some minor impurities.

For 20 Mer experiment:

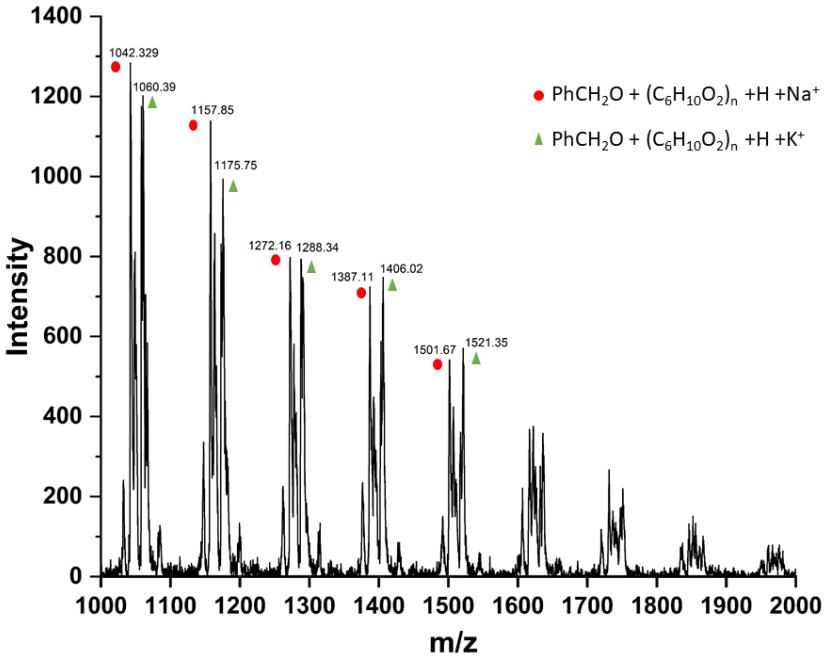

Figure S26: MALDI-TOF analysis of a dodecamer sample produced from the run of [CL]: [2]: [BnOH] as 20:1:2.

4. Crystallographic Data.

X-ray diffraction data of **1** and **2** were collected on a Rigaku XtaLAB Synergy, Dualflex four-circle diffractometer with HyPix3000 detector and Cu-K$_\alpha$ radiation (λ = 1.54184 Å) at 100 K. Data reduction was done with CrysAlis^{PRO}, Agilent Technologies, Version 1.171.37.34. The structures were solved by intrinsic phasing using SHELXT.[1] all refinements were carried out against F^2 with ShelXL[2] as implemented in the program system Olex 2.[3] The non-hydrogen atoms were refined with anisotropic displacement parameters. All hydrogen atoms were included in calculated positions and treated as riding throughout the refinement. Refinement results are given in Table S1. For both the crystals **1** and **2**, solvent masking was applied and potential solvent accessible area or void space was calculated using PLATON[4] executable in Olex 2. Graphical representations were performed with the program DIAMOND.[5] CCDC-2265706 **(1)** and CCDC- 2265707 **(2)** contain the supplementary crystallographic data for this paper. These data can be obtained free of charge from the Crystallographic Data Centre via www.ccdc.cam.ac.uk/data_request/cif using the CCDC numbers (given in the table) as reference.

Table S3: Crystallographic data of 1 and 2.

	1	**2**
Formula	$C_{32}H_{43}AlBrN_2O$	$C_{44}H_{59}AlN_2O$
Fw /g·mol^{-1}	661.61	658.91
crystal. colour, habit	Clear white	Clear white
crystal size / mm^3	0.71 × 0.43× 0.23	0.6 × 0.1 × 0.09
crystal system	monoclinic	monoclinic
space group	$P2_1/n$	$P2_1$
a / Å	14.48000(10)	12.6770(2)
b / Å	14.13040(10)	12.1215(2)
c / Å	16.53520(10)	13.1408(2)
α / °	90	90
β / °	100.9690(10)	98.944(2)
γ / °	90	90
V / Å^3	3321.43(4)	1994.72(6)
Z	4	2
ρ_{calc}/g·cm^{-3}	1.157	1.097
μ (CuKα)/mm^{-1}	2.117	0.688
F(000)	1220.0	716.0
2θ range / °	7.446 to 136.568	6.81 to 136.394
index ranges	-16 ≤ h ≤ 17, -16 ≤ k ≤ 16, -19 ≤ l ≤ 19	-15 ≤ h ≤ 15, -14 ≤ k ≤ 13, -15 ≤ l ≤ 15
Reflections collected	61920	21499
independ. reflns (R_{int})	6059 [R_{int} = 0.0780, R_{sigma} = 0.0260]	6326[R_{int} = 0.0691, R_{sigma} = 0.0491]
observed reflections	5916	5880
data/ restr./ param.	6059/0/338	6326/1/445
*R*1, *wR*2 [*I*> 2σ(*I*)]	R1 = 0.0395, wR2 = 0.1046	R1 = 0.0422, wR2 = 0.1157
*R*1, *wR*2 (all data)	R1 = 0.0401, wR2 = 0.1050	R1 = 0.0457, wR2 = 0.1202
GooF-of-fit on F^2	1.056	1.127
largest diff. peak, hole/ e·Å^3	0.74/-0.66	0.18/-0.24
CCDC number	2265706	2265707

5. DFT Calculation

All structures were optimized using M06-2X functional[6] using Gaussian 16 package.[7] The 6-31+G** basis set was used for H, C, O, N, Br and Al atoms, while LANL2DZ[8] was used for Ti for the geometry optimization. This basis set is referred as B1. All geometry optimizations were carried out in gas phase. The natures of the stationary points were characterized by frequency calculations at the same level of theory. The refinement of the energy was done by carrying out single-point energy calculations on the optimized structures using def2-TZVP basis set[9] (referred as B2) and M06-2X functional. The bonding in the given structures was analysed by Natural Bond Orbital (NBO)[10] methods at M06-2X/B2 level of theory. The Intrinsic Bond Strength Indices (IBSIs)[11] were calculated using Multiwfn.[12]

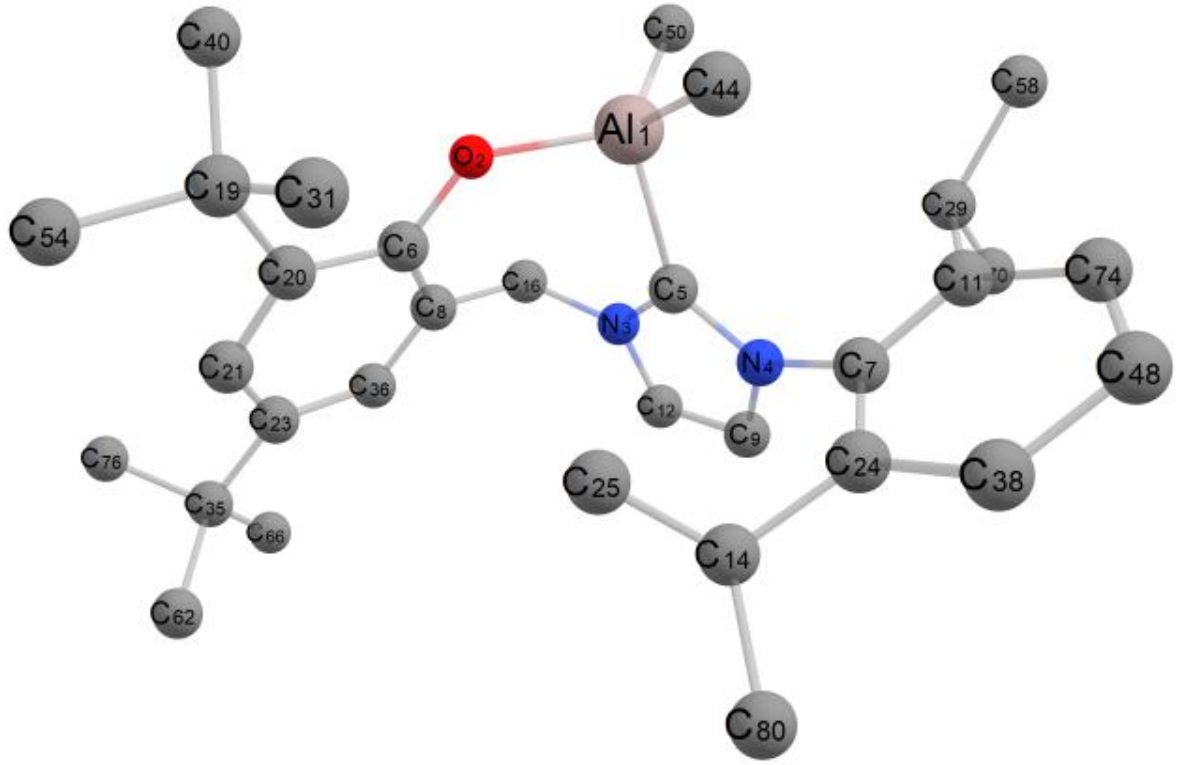

Figure S27: DFT optimized structure of Al-complex **2**. The hydrogen atoms are omitted for clarity.

Table S4: Comparison of the selected observed (from SCXRD data) versus computed (from DFT optimized geometry) bond distances (Å) and bond angles (º) for Al-complex.

Bond Length (Å)			
	obsd	calcd	Δ (calcd - obsd)
Al1-O2	1.77	1.80	0.03
Al1-C5	2.06	2.08	0.02
Al1-C44	1.97	1.98	0.01
Al1-C50	1.96	1.98	0.02

Bond Angle (º)			
	obsd	calcd	Δ (calcd - obsd)
∠O2-Al1-C5	100.5	97.1	-3.4
∠O2-Al1-C50	106.4	111.0	4.6
∠C5-Al1-C44	109.2	110.9	1.7
∠C5-Al1-C50	111.5	105.2	-6.3
∠C44-Al1-C50	115.2	115.9	0.7
∠O2-Al1-C44	112.9	114.6	1.7

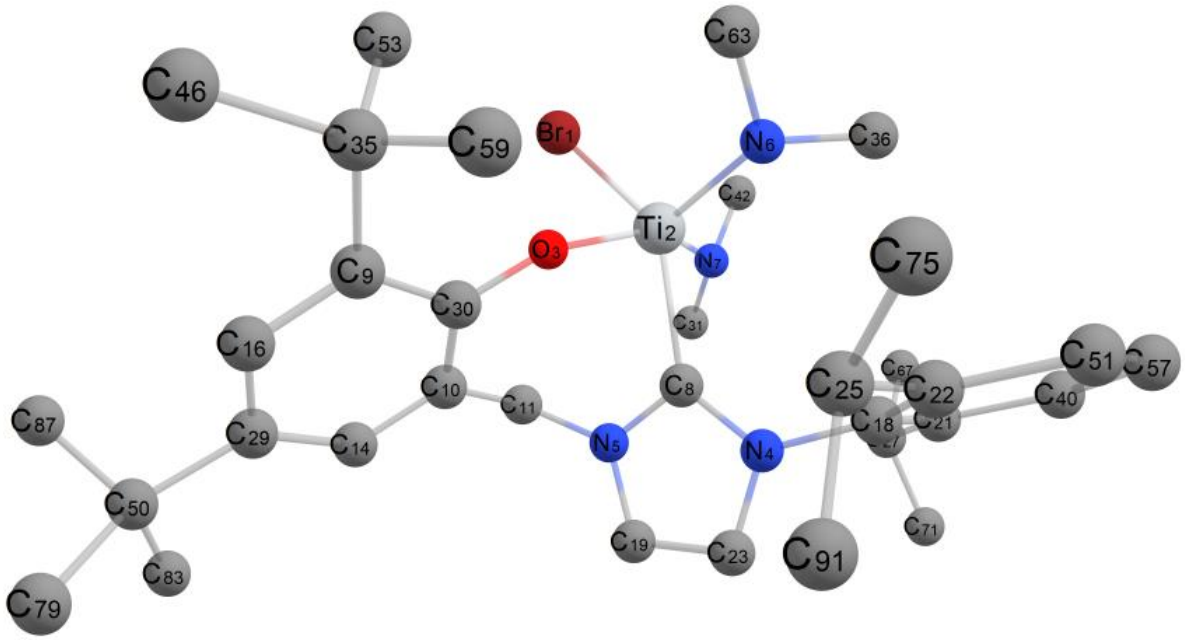

Figure S28: DFT optimized structure of Ti-complex [(L)Ti(NMe_2)$_2$Br]. The hydrogen atoms are omitted for clarity.

Table S5: Comparison of the selected observed (from SCXRD data) versus computed (from DFT optimized geometry) bond distances (Å) and bond angles (º) for Ti-complex.

Bond Length (Å)			
	obsd	calcd	Δ (calcd - obsd)
Ti2-Br1	2.57	2.52	-0.05
Ti2-O3	1.90	1.92	0.02
Ti2-N6	1.88	1.85	-0.03
Ti2-N7	1.94	1.92	-0.02
Ti-C8	2.23	2.22	-0.01

Bond Angle (º)			
	obsd	calcd	Δ (calcd - obsd)
∠C8–Ti2–Br1	150.5	141.9	-8.6
∠C8–Ti2–O3	80.6	79.1	-1.5
∠C8–Ti2–N6	106.0	109.8	3.8
∠C8–Ti2–N7	85.0	83.2	-1.8
∠N6–Ti2–N7	105.3	104.4	-0.9
∠N6–Ti2–O3	108.4	104.5	-3.9
∠N7–Ti2–O3	145.8	149.9	4.1
∠O3–Ti2–Br1	86.9	87.5	0.6
∠N6–Ti2–Br1	103.3	108.1	4.8
∠N7–Ti2–Br1	90.6	91.6	1.0

Cartesian Coordinates of the optimized structures of Al-complex and Ti-complex.

Al-complex

E=-1674.86651302 a.u.

13	1.073669000	1.731987000	-0.961747000
8	-0.720076000	1.830144000	-0.904854000
7	0.407897000	-1.068792000	-1.853092000
7	2.054192000	-1.233888000	-0.498422000
6	1.213254000	-0.337222000	-1.060389000
6	-1.755697000	1.006646000	-0.745971000
6	3.012490000	-0.881301000	0.518505000
6	-1.856186000	-0.168040000	-1.518626000
6	1.782213000	-2.515134000	-0.942013000
1	2.350087000	-3.368586000	-0.605867000
6	4.220701000	-0.288420000	0.127448000
6	0.728723000	-2.408823000	-1.794430000
1	0.190190000	-3.157834000	-2.353391000
6	1.284188000	-1.654660000	2.235069000
1	0.969708000	-2.349693000	1.449238000
6	-0.774069000	-0.485897000	-2.515920000
1	-1.120702000	-1.214696000	-3.251877000
1	-0.440355000	0.412827000	-3.041845000
6	-2.767139000	2.599676000	1.003049000
6	-2.798782000	1.308738000	0.173714000
6	-3.846122000	0.396771000	0.288690000
1	-4.640851000	0.618187000	0.992595000
6	-3.947295000	-0.791766000	-0.451667000
6	2.650796000	-1.098203000	1.857521000
6	0.239869000	-0.528127000	2.299830000
1	0.522033000	0.208409000	3.060996000
1	-0.743532000	-0.935136000	2.558348000
1	0.139302000	0.000685000	1.347101000
6	4.558593000	-0.074292000	-1.339284000

1	3.623539000	0.113804000	-1.878573000
6	-1.544149000	2.594128000	1.937695000
1	-1.606159000	1.754117000	2.639035000
1	-1.516782000	3.522267000	2.520676000
1	-0.610305000	2.513694000	1.379729000
6	-5.145326000	-1.720924000	-0.238725000
6	-2.930561000	-1.047969000	-1.363010000
1	-2.955339000	-1.939171000	-1.985213000
6	3.574991000	-0.716794000	2.833050000
1	3.339228000	-0.862072000	3.881803000
6	-2.715667000	3.823716000	0.069063000
1	-1.826345000	3.806594000	-0.561105000
1	-2.707207000	4.742689000	0.666544000
1	-3.600728000	3.845984000	-0.576241000
6	1.986881000	2.424400000	0.648409000
1	1.696065000	3.463043000	0.851874000
1	3.074629000	2.424947000	0.495333000
1	1.797156000	1.850164000	1.563308000
6	4.789619000	-0.137911000	2.479351000
1	5.490083000	0.158798000	3.253813000
6	1.766546000	2.384219000	-2.701289000
1	1.508761000	1.745319000	-3.556114000
1	2.861276000	2.470644000	-2.686292000
1	1.375495000	3.384512000	-2.925616000
6	-4.015531000	2.749760000	1.883973000
1	-4.934337000	2.783994000	1.288431000
1	-3.944913000	3.689708000	2.440528000
1	-4.102610000	1.938531000	2.615012000
6	5.461071000	1.138267000	-1.577600000
1	6.476254000	0.968751000	-1.203583000
1	5.058789000	2.035370000	-1.097215000
1	5.536417000	1.332268000	-2.651369000

6	-5.178240000	-2.190327000	1.226588000
1	-4.261484000	-2.733915000	1.478000000
1	-6.032705000	-2.855846000	1.394486000
1	-5.268723000	-1.346004000	1.916459000
6	-5.076969000	-2.961110000	-1.136765000
1	-5.084224000	-2.690777000	-2.198067000
1	-5.947186000	-3.598277000	-0.949083000
1	-4.178660000	-3.554719000	-0.935227000
6	5.192925000	-1.345358000	-1.924091000
1	5.417279000	-1.207369000	-2.986316000
1	4.526498000	-2.207713000	-1.825095000
1	6.127565000	-1.576570000	-1.401411000
6	5.108347000	0.075496000	1.142687000
1	6.052579000	0.544312000	0.887092000
6	-6.448608000	-0.967702000	-0.559135000
1	-6.576181000	-0.093222000	0.085802000
1	-7.313718000	-1.624188000	-0.411404000
1	-6.449058000	-0.622347000	-1.597946000
6	1.299905000	-2.436026000	3.552025000
1	2.090283000	-3.192615000	3.566218000
1	0.338808000	-2.938981000	3.690858000
1	1.443756000	-1.772975000	4.411203000

Ti-complex

E=-5045.45096599 a.u.

35	-0.316872000	3.592306000	-0.972694000
22	0.801620000	1.438376000	-0.285421000
8	-0.927757000	0.815282000	0.272897000
7	1.730588000	-1.743084000	-0.477947000
7	0.040644000	-1.238630000	-1.683324000
7	1.720264000	1.745556000	1.301191000
7	2.133354000	1.631440000	-1.651320000

6	0.934728000	-0.708392000	-0.826396000
6	-3.176470000	0.240280000	0.875676000
6	-2.236998000	-0.424377000	-1.270628000
6	-1.076707000	-0.451608000	-2.223387000
1	-1.364102000	-0.892652000	-3.181000000
1	-0.694128000	0.558458000	-2.424995000
6	-3.434954000	-1.055914000	-1.611079000
1	-3.499609000	-1.540296000	-2.581725000
6	-4.348266000	-0.403530000	0.486491000
1	-5.187094000	-0.394136000	1.173966000
6	2.858275000	-1.657189000	0.412407000
6	0.261769000	-2.588206000	-1.879797000
1	-0.358297000	-3.189948000	-2.525593000
6	4.137727000	-1.558657000	-0.148436000
6	2.627980000	-1.691145000	1.799510000
6	1.340129000	-2.909401000	-1.121535000
1	1.859338000	-3.842814000	-0.970965000
6	1.220230000	-1.752290000	2.373370000
1	0.579158000	-1.117282000	1.748683000
6	4.367222000	-1.456155000	-1.645617000
1	3.397223000	-1.311908000	-2.131587000
6	-4.519475000	-1.060739000	-0.742090000
6	-2.080900000	0.227618000	-0.032218000
6	2.162639000	1.111625000	-3.003741000
1	1.726790000	0.110652000	-3.060009000
1	3.195503000	1.053596000	-3.379387000
1	1.602854000	1.769390000	-3.689200000
6	-3.063154000	0.959032000	2.222875000
6	3.160126000	1.728327000	1.489063000
1	3.650555000	1.248908000	0.637498000
1	3.416792000	1.161305000	2.395447000
1	3.554024000	2.749938000	1.603721000

6	5.228768000	-1.550271000	0.727438000
1	6.235756000	-1.483590000	0.326143000
6	2.847703000	2.905622000	-1.606832000
1	2.416402000	3.623279000	-2.319974000
1	3.908847000	2.751782000	-1.858169000
1	2.789773000	3.363826000	-0.616340000
6	-4.339894000	0.828405000	3.064161000
1	-5.205787000	1.274919000	2.564405000
1	-4.195906000	1.358964000	4.011013000
1	-4.571569000	-0.216501000	3.298720000
6	-5.857481000	-1.729261000	-1.066184000
6	3.751355000	-1.677499000	2.628973000
1	3.622926000	-1.701897000	3.705323000
6	-2.821346000	2.460996000	1.978942000
1	-1.976272000	2.640941000	1.312285000
1	-2.640770000	2.972340000	2.932514000
1	-3.705885000	2.910571000	1.515373000
6	5.038878000	-1.619456000	2.100715000
1	5.895602000	-1.613702000	2.767548000
6	-1.915643000	0.338754000	3.040847000
1	-2.135626000	-0.714738000	3.253911000
1	-1.804840000	0.864640000	3.997485000
1	-0.967165000	0.390722000	2.504923000
6	1.015933000	2.399542000	2.396000000
1	1.364729000	3.436850000	2.503095000
1	1.188414000	1.873663000	3.345546000
1	-0.058840000	2.423905000	2.204277000
6	5.232570000	-0.237797000	-1.985850000
1	4.782658000	0.674722000	-1.582556000
1	5.323591000	-0.130759000	-3.071426000
1	6.243696000	-0.336107000	-1.578039000
6	4.991454000	-2.745638000	-2.194730000

1	5.971574000	-2.926019000	-1.739933000
1	5.128663000	-2.672723000	-3.277986000
1	4.360913000	-3.615535000	-1.986445000
6	1.147173000	-1.212552000	3.803089000
1	1.647045000	-1.881530000	4.512113000
1	0.102915000	-1.129219000	4.113702000
1	1.605634000	-0.221862000	3.880512000
6	-6.163630000	-2.808550000	-0.012779000
1	-7.120909000	-3.294276000	-0.233417000
1	-6.227104000	-2.382112000	0.992738000
1	-5.380640000	-3.573854000	-0.005219000
6	-5.846591000	-2.396460000	-2.445945000
1	-5.083454000	-3.179838000	-2.508338000
1	-5.664201000	-1.668849000	-3.243814000
1	-6.818943000	-2.862284000	-2.635346000
6	-6.977175000	-0.673467000	-1.051798000
1	-7.941811000	-1.139215000	-1.283336000
1	-6.781559000	0.106698000	-1.794258000
1	-7.062291000	-0.191965000	-0.073093000
6	0.667738000	-3.185250000	2.332740000
1	0.633063000	-3.582718000	1.315487000
1	-0.349749000	-3.205395000	2.735620000
1	1.292839000	-3.848935000	2.940750000

6. References.

1. G. Sheldrick, *Acta Crystallogr., Sect. A: Found. Adv.*, 2015, **71**, 3-8.
2. G. Sheldrick, *Acta Crystallogr., Sect. C: Struct. Chem.*, 2015, **71**, 3-8.
3. O. V. Dolomanov, L. J. Bourhis, R. J. Gildea, J. A. K. Howard and H. Puschmann, *J. Appl. Crystallogr.*, 2009, **42**, 339-341.
4. A. Spek, *Acta Crystallogr., Sect. D*, 2009, **65**, 148-155.
5. K. Brandenburg, Diamond Version 4.6.0, Crystal Impact GbR, Bonn, 2019.
6. Y. Zhao and D. G. Truhlar, *Theor. Chem. Acc.*, 2008, **120**, 215-241.
7. Gaussian 16, Revision B.01, M. J. Frisch, G. W. Trucks, H. B. Schlegel, G. E. Scuseria, M. A. Robb, J. R. Cheeseman, G. Scalmani, V. Barone,; G. A. Petersson, H. Nakatsuji, X. Li, M. Caricato, A. V. Marenich, J. Bloino, B. G. Janesko, R. Gomperts, B. Mennucci, H. P. Hratchian, J. V. Ortiz, A. F. Izmaylov, J. L. Sonnenberg, D. Williams-Young, F. Ding, , F. Lipparini, F. Egidi, J. Goings, B.

Peng, A. Petrone, T. Henderson, D. Ranasinghe, V. G. Zakrzewski, J. Gao, N. Rega, G. Zheng, W. Liang, M. Hada, M. Ehara, K. Toyota, R. Fukuda, J. Hasegawa, M. Ishida, T. Nakajima, Y. Honda, O. Kitao, H. Nakai, T. Vreven, K. Throssell, J. A. Montgomery Jr., J. E. Peralta, F. Ogliaro, M. J. Bearpark, J. J. Heyd, E. N. Brothers, K. N. Kudin, V. N. Staroverov, T. A. Keith, R. Kobayashi, J. Normand, K. Raghavachari, A. P. Rendell, J. C. Burant, S. S. Iyengar, J. Tomasi, M. Cossi, J. M. Millam, M. Klene, C. Adamo, R. Cammi, J. W. Ochterski, R. L. Martin, K. Morokuma, O. Farkas, J. B. Foresman, D. J. Fox, Gaussian, Inc., Wallingford CT (2016) Wallingford, U.S.A.

8. (a) P. J. Hay and W. R. Wadt, *J. Chem. Phys.*, 1985, **82**, 270-283; (b) W. R. Wadt and P. J. Hay, *J. Chem. Phys.*, 1985, **82**, 284-298; (c) P. J. Hay and W. R. Wadt, *J. Chem. Phys.* 1985, **82**, 299-310.
9. (a) F. Weigend and R. Ahlrichs, *Phys. Chem. Chem. Phys.*, 2005, **7**, 3297-3305; (b) F. Weigend, M. Häser, H. Patzelt and R. Ahlrichs, *Chem. Phys. Lett.*, 1998, **294**, 143-152.
10. A. E. Reed, L. A. Curtiss and F. Weinhold, *Chem. Rev.*, 1988, **88**, 899-926.
11. J. Klein, H. Khartabil, J.-C. Boisson, J. Contreras-García, J.-P. Piquemal and E. Hénon, . *Phys. Chem. A*, 2020, **124**, 1850-1860.
12. T. Lu and F. Chen, *J. Comput. Chem.*, 2012, **33**, 580-592.